Acta Crystallographica Section A
Foundations of Crystallography
ISSN 0108-7673

Received 6 August 2008
Accepted 16 September 2008

On the determination of fiber tilt angles in fiber diffraction

Norbert Stribeck

Institute of Technical and Macromolecular Chemistry, Department of Chemistry, University of Hamburg, Bundesstrasse 45, 20146 Hamburg, Germany. Correspondence e-mail: norbert@stribeck.de

The common digital method that is used to eliminate the effect of fiber tilt from fiber diffraction patterns is based on an approximation given by Franklin & Gosling [*Acta Cryst.* (1953), **6**, 678–685]. The estimate of the tilt angle is iteratively optimized in the so-called 'Fraser correction'. Building on the fundamental work of Polanyi [*Z. Phys.* (1921), **7**, 149–180], the exact solution is presented.

1. Introduction

Each quantitative analysis of a two-dimensional diffraction pattern with fiber symmetry starts with a geometric correction. This transformation remaps the detector image onto a plane of reciprocal space $\mathbf{s} = (s_1, s_2, s_3)$ that contains the meridian, s_3. The magnitude of the scattering vector is defined by $|\mathbf{s}| = s = (2/\lambda)\sin\theta$. λ is the wavelength of radiation and 2θ is the scattering angle. Fiber symmetry means that the scattering intensity $I(\mathbf{s}) = I(s_{12}, s_3)$ exhibits cylindrical symmetry, with $s_{12} = (s_1^2 + s_2^2)^{1/2}$.

At least two recently published open-source computer programs (Rajkumar *et al.*, 2005; Bian *et al.*, 2006) offer the common (Fraser *et al.*, 1976) digital correction method ('Fraser correction'), which involves several steps. The subject of this communication is the first nontrivial step, in which both the tilt angle β of the fiber with respect to the plane perpendicular to the primary beam and the position of the primary beam on the detector are refined interactively (Fraser *et al.*, 1976), even if images of sharp reflections in the pattern could be used for direct computation. In the Fraser process this iteration is essential, because the inversion equation of Franklin & Gosling (1953) has proved (Fraser *et al.*, 1976; Millane & Arnott, 1985) to return approximations only. Here it will be demonstrated that the exact solution is obtained by simple analysis of the scattering geometry. Just like in the cited original work, for this purpose the positions of three or four image spots of the same reflection are employed.

An attempt to study the position of these image spots in the tilted fiber diagram without a sophisticated abstraction of the problem may cause rather complex equations. An ingenious abstraction has been presented by Polanyi (1921) in an obviously forgotten work. It is based on the intersection of two spheres and results in the Polanyi equations. Inversion of the Polanyi equations returns analytical expressions for the tilt angle β.

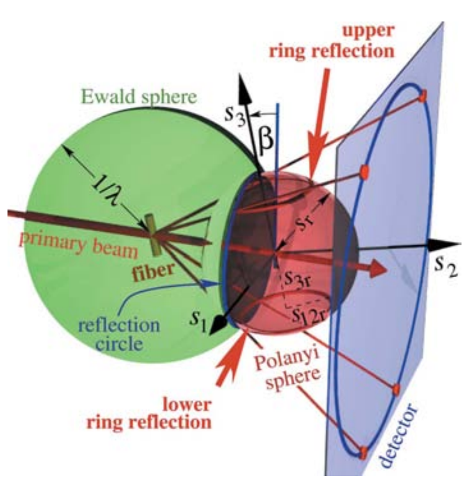

Figure 1
Sketch of fiber diffraction geometry with Ewald sphere and Polanyi sphere. The curve of intersection is a circle ('reflection circle') that does not change as the fiber is tilted (tilt angle β). The radius of the Polanyi sphere is chosen to match the magnitude s_r of a chosen reflection manifested in two rings $(s_{12r}, \pm s_{3r})$. The trihedron (s_1, s_2, s_3) indicates reciprocal space.

2. Theoretical

Assumption. Let the fiber diffraction experiment be carried out in normal transmission geometry using a flat two-dimensional detector; the detector tilt be determined in a test experiment using an isotropic sample with sharp reflections; and the patterns be corrected accordingly.

2.1. Polanyi construction and direction angles

Polanyi (1921) considers only reflections that diffract under a single scattering angle $2\theta_r$. Thus, in reciprocal space their images are on a sphere about the origin that has the radius s_r. On this Polanyi sphere ($|\mathbf{s}_r| = s_r$), let us consider one special fiber reflection with $\mathbf{s}_r = (s_{12r}, \pm s_{3r})$, which becomes manifest in two thin rings. In Fig. 1 short thick arrows point at these ring reflections.

The fiber is irradiated by the primary beam and the corresponding cross section defines the center of the Ewald sphere of radius $1/\lambda$. Where the primary beam exits from the Ewald sphere, the origin of reciprocal space is located (axes s_1, s_2 and s_3). A plane two-dimensional detector probes the surface of the Ewald sphere. Thus, the intersection of the surfaces of the Ewald sphere and the Polanyi sphere is the curve from which intensity of the chosen reflection can reach the detector. Polanyi calls this curve the reflection circle. As the fiber in the primary beam is tilted by the angle β, the Polanyi sphere together with reciprocal space are rotating similarly. Nevertheless, the position of the reflection circle remains the same with respect to the primary beam and the detector. The reflection circle itself is mapped onto the detector plane by central projection. Fig. 1 demonstrates a case in which all four possible image spots appear on the detector. Obviously, contraction of the rings on the sphere will cause image spots to vanish on the detector. A sketch of the detector plane is presented in Fig. 2.

As long as the positions of at least three image spots of any reflection on the detector can be measured accurately, the center of the reflection circle is determined. A principal uncertainty as alleged by Fraser *et al.* (1976) does not exist. The meridional axis f_3 in the 'film' coordinate system is always a symmetry axis, and the equatorial axis f_1 runs in the perpendicular direction through the center of the reflection circle. Only an ideal ($\beta = 0$) fiber diagram exhibits four-quadrant symmetry. In this case, the four image spots of the reflection are found under the uniform direction angle δ_0, which is measured against the meridional axis. As demonstrated by Polanyi, this angle is given by $\cos\delta_0 = \cos\rho/\cos\theta_r$ with $\cos\rho = s_{3r}/s_r$. This 'ideal Polanyi equation' is readily established by consideration of a spherical triangle on the Polanyi sphere and application of the cosine rule for sides. As a function of the tilt angle β, the image spots move on the reflection circle and can disappear or appear on the meridian. For the tilted fiber diagram the deduction of the direction angle δ is similar to that for the ideal fiber diagram and gives the general Polanyi equation

$$\cos\delta = \frac{\cos\rho - \sin\beta\,\sin\theta_r}{\cos\beta\,\cos\theta_r}. \quad (1)$$

As it is written here, the equation looks different from that published in the original paper (Polanyi, 1921), because Polanyi defines $\beta_{\rm Polanyi} = \pi/2 - \beta$ by the angle between the fiber and primary beam, whereas here the currently customary tilt-angle definition is used. If δ is called the 'upper' direction angle, then the general Polanyi equation for the lower direction angle δ' is obtained by the substitution $\beta \rightarrow -\beta$:

$$\cos\delta' = \frac{\cos\rho + \sin\beta\,\sin\theta_r}{\cos\beta\,\cos\theta_r}. \quad (2)$$

2.2. Inversion of the Polanyi equations

Let us leave the paper of Polanyi and turn to the determination of the tilt angle β. Solving equations (1) and (2) directly for $\cos\beta$ gives

$$\cos\beta = \frac{\cos\rho}{\cos\theta_r}\,\frac{2}{\cos\delta + \cos\delta'}. \quad (3)$$

Equation (3) is numerically stable for small tilt angle (*i.e.* $\cos\delta \simeq \cos\delta'$), because it contains the sum but not the difference of the measured direction angle cosines. On the other hand, the sign of the tilt angle is lost. Let the equation be converted for practical use. From the crystal structure data $\cos\rho = s_{3r}/s_r$ can be computed. With $\sin\theta_r = (\lambda s_r)/2$ from the definition of the magnitude of the scattering vector, and $\cos\theta_r = (1 - \lambda^2 s_r^2/4)^{1/2}$, it follows that

$$\cos\beta = \frac{s_{3r}}{s_r(4 - \lambda^2 s_r^2)^{1/2}}\,\frac{4}{\cos\delta + \cos\delta'}. \quad (4)$$

It should be mentioned that the angle δ' is measured against the negative branch of the meridional axis (*cf.* Fig. 2).

Franklin & Gosling (1953) [their equation (5)] report a simple equation,

$$\tan\beta = (s_{3r} + s'_{3r})/(\lambda s_r^2), \quad (5)$$

without deduction, which has turned out to be inaccurate (Fraser *et al.*, 1976; Millane & Arnott, 1985). Moreover, the relation to measurable numbers is somewhat awkward. Thus, in Fig. 2 the measurable vertical components f_{3r} and f'_{3r} have been drawn in. Upon central back-projection onto the reflection circle they turn into s_{3r} and s'_{3r}. In order to compute these components, the distance between the sample and the detector must be known – which is unnecessary, in principle.

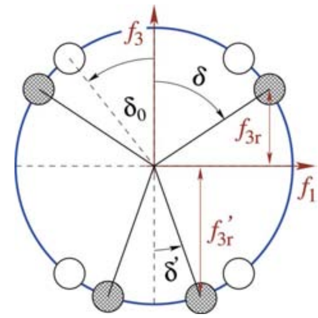

Figure 2
Image positions of a specific fiber reflection on a plane detector (after Polanyi, 1921). Open symbols mark the positions for a fiber oriented perpendicular to the primary beam (direction angle δ_0). Filled symbols mark typical positions for a tilted fiber. The direction angles δ and δ' determine the tilt angle β of the fiber.

By subtracting the general Polanyi equations from each other, the solution sought by Franklin and Gosling is readily established:

$$\tan\beta = \frac{2\cos\theta_r}{\sin\theta_r}(\cos\delta' - \cos\delta) = \frac{(4 - \lambda^2 s_r^2)^{1/2}}{2\lambda s_r}(\cos\delta' - \cos\delta). \quad (6)$$

The equation published by Franklin & Gosling (1953) [*i.e.* equation (5)] is obtained by substituting $\cos\delta' = -s'_{3r}/s_3$ and $\cos\delta = s_{3r}/s_3$, and replacing $\cos\theta_r = 1$ for all θ_r.

Although application to model fiber diffraction patterns with spot-shaped reflections and small tilt angles confirms an advantage of the cosine relation over the tangent relation, the advantage is turned into a severe disadvantage when arc-shaped reflections of real patterns are processed. In this case the observed direction angles appear shifted in the same direction, and only equation (6) returns a tilt angle that can be accepted for a direct mapping without tilt-angle refinement.

3. Conclusion

The exact inversion equation for the tilt angle β remedies a substantial handicap concerning the direct mapping of two-dimensional fiber scattering patterns onto the reciprocal space. Admittedly, iterative refinement of the mapping parameters is the best way to obtain high-quality intensity maps in reciprocal space, as long as the procedure is based on proper consideration of diffraction geometry. Thus, in static crystallographic studies the available interactive computer programs are the methods of choice. Nevertheless, in time-resolved scattering experiments many patterns must be preprocessed and evaluated. Practical application will show in which kind of investigations the time-consuming refinement of transformation parameters that is typical for the current Fraser-correction method can be avoided. Moreover, the abstraction of Polanyi may help to devise fast mapping procedures based on the geometrical properties of the reflection circle.

References

Bian, W., Wang, H., McCullough, I. & Stubbs, G. (2006). *J. Appl. Cryst.* **39**, 752–756.
Franklin, R. E. & Gosling, R. G. (1953). *Acta Cryst.* **6**, 678–685.
Fraser, R. D. B., Macrae, T. P., Miller, A. & Rowlands, R. J. (1976). *J. Appl. Cryst.* **9**, 81–94.
Millane, R. P. & Arnott, S. (1985). *J. Macromol. Sci. Phys. B*, **24**, 193–227.
Polanyi, M. (1921). *Z. Phys.* **7**, 149–180.
Rajkumar, G., AL-Khayat, H., Eakins, F., He, A., Knupp, C. & Squire, J. (2005). *Fibre Diffr. Rev.* **13**, 11–18.